 Human Molecular Genetics, 1999, Vol. 8, No. 2 345–352

A novel protein tyrosine phosphatase gene is mutated in progressive myoclonus epilepsy of the Lafora type (EPM2)

José M. Serratosa[1,*], Pilar Gómez-Garre[1], Mª Esther Gallardo[2,3], Berta Anta[1], Daniel Beltrán-Valero de Bernabé[2,3], Dick Lindhout[4], Paul B. Augustijn[5], Carlo A. Tassinari[6], Roberto Michelucci[6], Alain Malafosse[7], Meral Topcu[8], Djamel Grid[9], Charlotte Dravet[10], Samuel F. Berkovic[11] and Santiago Rodríguez de Córdoba[2,3]

[1]Laboratorio y Servicio de Neurología and [2]Unidad de Patología Molecular, Fundación Jiménez Díaz, Avenida Reyes Católicos 2, 28040 Madrid, Spain, [3]Departamento de Inmunología, Centro de Investigaciones Biológicas, Consejo Superior de Investigaciones Científicas, Velázquez 144, 28006 Madrid, Spain, [4]MGC Department of Clinical Genetics, Erasmus Universiteit Rotterdam, Rotterdam, The Netherlands, [5]Instituut voor Epilepsiebestrijding 'Meer en Bosch'–'De Cruquiushoeve', Heemstede, The Netherlands, [6]Divisione di Neurologia, Ospedale Bellaria, Bologna, Italy, [7]Division of Neuropsychiatry, Hospital Belle-Idee, University of Geneva Medical School, Geneve, Switzerland, [8]Department of Child Neurology, Hacettepe Children's Hospital, Ankara, Turkey, [9]Généthon, Evry, France, [10]Centre Saint Paul, Marseille, France and [11]Department of Medicine (Neurology), Austin and Repatriation Medical Center, Melbourne, Australia

Received September 29, 1998; Revised and Accepted November 16, 1998 DDBJ/EMBL/GenBank accession nos AJ130763, AJ130764

Progressive myoclonus epilepsy of the Lafora type or Lafora disease (EPM2; McKusick no. 254780) is an autosomal recessive disorder characterized by epilepsy, myoclonus, progressive neurological deterioration and glycogen-like intracellular inclusion bodies (Lafora bodies). A gene for EPM2 previously has been mapped to chromosome 6q23–q25 using linkage analysis and homozygosity mapping. Here we report the positional cloning of the 6q EPM2 gene. A microdeletion within the EPM2 critical region, present in homozygosis in an affected individual, was found to disrupt a novel gene encoding a putative protein tyrosine phosphatase (PTPase). The gene, denoted *EPM2*, presents alternative splicing in the 5′ and 3′ end regions. Mutational analysis revealed that EPM2 patients are homozygous for loss-of-function mutations in *EPM2*. These findings suggest that Lafora disease results from the mutational inactivation of a PTPase activity that may be important in the control of glycogen metabolism.

INTRODUCTION

The epilepsies constitute one of the most common neurological disorders, affecting 1–3% of the population (1,2). Among the epilepsies, the progressive myoclonus epilepsies (PMEs) constitute a rare, heterogeneous group characterized by the presence of myoclonus, seizures and progressive neurological deterioration (3). PME with polyglucosan intracellular inclusion bodies (EPM2) was first described in 1911 by Gonzalo R. Lafora (4,5). He originally called the inclusion bodies 'intracellular amyloid bodies' when he observed them in the brain and spinal cord of an adolescent patient who presented a progressive and fatal myoclonic epilepsy. In 1955, Harriman and Millar showed that the inclusions were not limited to the central nervous system and described similar intracellular inclusions in the heart and liver of one patient affected with PME (6). Also in 1955, Lafora suggested that the disease he had described almost half a century before could possibly be a generalized storage disorder and that it might be related to the glycogenoses (7).

EPM2 is inherited as an autosomal recessive trait. Linkage analysis and homozygosity mapping have localized a gene for EPM2 to a 2.7 cM region in chromosome 6q23–25 flanked by *D6S1003* and *D6S311* (8,9). Five microsatellite markers (*D6S1010*, *D6S1049*, *D6S1703*, *D6S1042* and *D6S978*) were found to be included within the critical region (9). However, there is evidence supporting genetic heterogeneity with at least a second locus responsible for a minority of EPM2 families (10).

RESULTS AND DISCUSSION

We have identified a patient (FD-3), born to a consanguineous marriage, with EPM2 and complete loss of the *D6S1703* microsatellite marker. Analysis of *D6S1703* alleles in the members of family FD is consistent with the presence of a null allele segregating with the disease (Fig. 1). A vectorette-PCR

*To whom correspondence should be addressed. Tel: +34 91 550 4854; Fax: +34 91 549 7381; Email: serratosa@jet.es

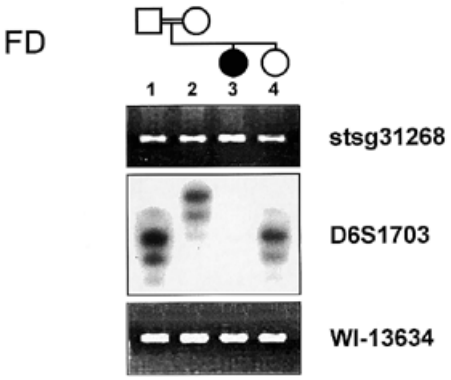

Figure 1. Homozygous deletion within the EPM2 critical region. Relevant portions of gels showing the typing of the non-polymorphic STS markers stsg31268 and WI-13634 (ethidium bromide-stained agarose gels) and the microsatellite marker *D6S1703* (polyacrylamide sequencing gel) in family FD. The affected individual is identified in the pedigree with a solid symbol. Segregation of the *D6S1703* marker in this family indicates that both parents are heterozygous for a *D6S1703* null allele.

strategy (11,12) was used to amplify the genomic sequences flanking *D6S1703* from normal human genomic DNA. We obtained PCR fragments that overlap and extend both ends of *D6S1703*. The PCR fragments flanking *D6S1703* are also lost in the genomic DNA of FD-3, excluding the possibility that the loss of *D6S1703* in the patient was a consequence of primer mismatch due to a point mutation. These data indicate that FD-3 is homozygous for a microdeletion in the EPM2 critical region and suggest that the phenotype may result from the disruption of a gene adjacent to *D6S1703*.

The PCR fragments flanking *D6S1703* were used as probes to screen cosmid and phage P1-derived artificial chromosome (PAC) human genomic libraries. Several overlapping clones were identified and characterized by restriction endonuclease digestion, Southern blot hybridization, PCR and sequence analyses. These clones organize a contig that encompasses the deletion in patient FD-3 (Fig. 2A). To identify the deletion breakpoints, we designed several amplimers along the contig and tested them by PCR in DNA of the patient presenting the homozygous deletion. During the course of these experiments, the Sanger Centre (Cambridgeshire, UK) released the complete nucleotide sequence of a 150 kb clone (466P17) including *D6S1703* and encompassing the deletion. These sequence data facilitated the accurate localization of the breakpoints and provided us with the complete sequence of the 60 kb DNA fragment that is lost in FD-3.

A search of the expressed sequence tag (EST) database with this 60 kb nucleotide sequence identified a human testis 986 bp cDNA sequence (zu70h03). The nucleotide sequence of zu70h03 does not contain any open reading frame (ORF) of significant length. Alignment of the nucleotide sequences of the 150 kb 466P17 clone and zu70h03 revealed that the first 595 nucleotides of zu70h03 are arranged in six exons (a, 2a, 2b, b, c and d) located within the 60 kb DNA fragment that is deleted in FD-3. The last 391 nucleotides of zu70h03, encoded by a separate exon named 3a, were mapped by long distance-PCR (LD-PCR) to PAC3, outside the deleted region (Fig. 2A and B).

In an attempt to isolate a full-length cDNA, we screened human brain (hippocampus, fetal brain and adult brain) and testis cDNA libraries with probes derived from zu70h03. We also searched the EST databases with the nucleotide sequence of zu70h03. These analyses resulted in the identification of additional cDNA clones. Four of them (DKFZp596H2425Q2, yx64g05, aa52d08 and yg02h03) were fully sequenced in both strands. Exon organization of these clones was analyzed by sequence comparison between them and with the sequence of clone 466P17 (Fig. 2A and B). Exon entities were confirmed by PCR using normal human genomic DNA. Careful examination of the exon organization of the DKFZp596H2425Q2, yx64g05, aa52d08 and yg02h03 clones indicated that they are transcripts (also incomplete) that result from the alternative splicing of the same gene. Additional nucleotide sequences upstream of the most 5′ end of the cDNA clones described above were obtained by PCR amplification from a human fetal liver cDNA library (λDR2-A; Fig. 2B).

RT–PCR amplification using human liver and skeletal muscle mRNA was used to determine the exon composition of the *EPM2* transcript in these tissues (Fig. 2B). Only primers derived from exons 1, 2, 3 and 4 resulted in amplification of *EPM2* PCR products, suggesting that the *EPM2* exons a, 2a, 2b, b, c, d and 3a are not present in the majority of the *EPM2* transcripts in these tissues. The information obtained from these RT–PCR fragments was used to assemble a composite cDNA describing the organization of the *EPM2* transcript (Fig. 2C).

By northern blot hybridization using the yx64g05 EST as a probe, we detected transcription of the *EPM2* candidate gene as a single mRNA band of ~3 kb in length in different adult human tissues (Fig. 3).

The composite sequence of the *EPM2* positional candidate gene depicted in Figure 2C contains two alternative ORFs of 250 amino acids (exons 1, 2, 3 and 4) and 236 amino acids (exons 1, 2, 3, 4a and 4b) (Fig. 4A). These ORFs seem to be incomplete at their N-terminal ends, suggesting that the translation start ATG codon is located within a yet to be identified exon upstream of exon 1. The *EPM2* ORFs were compared by BLAST analysis with sequences deposited in pertinent databases. This analysis demonstrated that the amino acid sequence encoded by exon 4a is 25–37% identical (in a 64 amino acid ungapped alignment) to the amino acid sequence of protein tyrosine phosphatases (PTPases) from different species. All PTPases have a conserved catalytic domain with a unique motif (I/V)HCxAGxxR(S/T)G (x = any amino acid) in which the cysteine residue is critical for enzyme function (13). This motif is conserved in the putative protein encoded by the candidate gene for EMP2 (Fig. 4). We postulate that the positional candidate gene for EPM2 encodes a PTPase. We denoted this protein as LAFPTPase (from LAFora PTPase). No other similarities were found between sequences in the databases and the LAFPTPase amino acid sequence.

We have shown above that the EPM2 patient in family FD presents a 60 kb deletion in homozygosis (*EPM2*-60kbdel) that disrupts the *EPM2* gene. Characterization of the genomic organization of the *EPM2* transcript (Fig. 2 and C) illustrates that transcription of the *EPM2* gene in patient FD-3 would result in a *EPM2* transcript that lacks exon 2. Deletion of exon 2 causes an ORF frameshift that generates a stop codon within exon 3. *EPM2*-60kbdel is, therefore, a loss-of-function mutation.

To determine whether the *EPM2* gene is also mutated in other EPM2 families, we performed a mutational analysis by single strand conformation polymorphism (SSCP). One family (S114) with band-shifts in exon 2, two families (S2 and S12) with band-shifts in exon 3 and five families (F38, S109, F119, F95 and

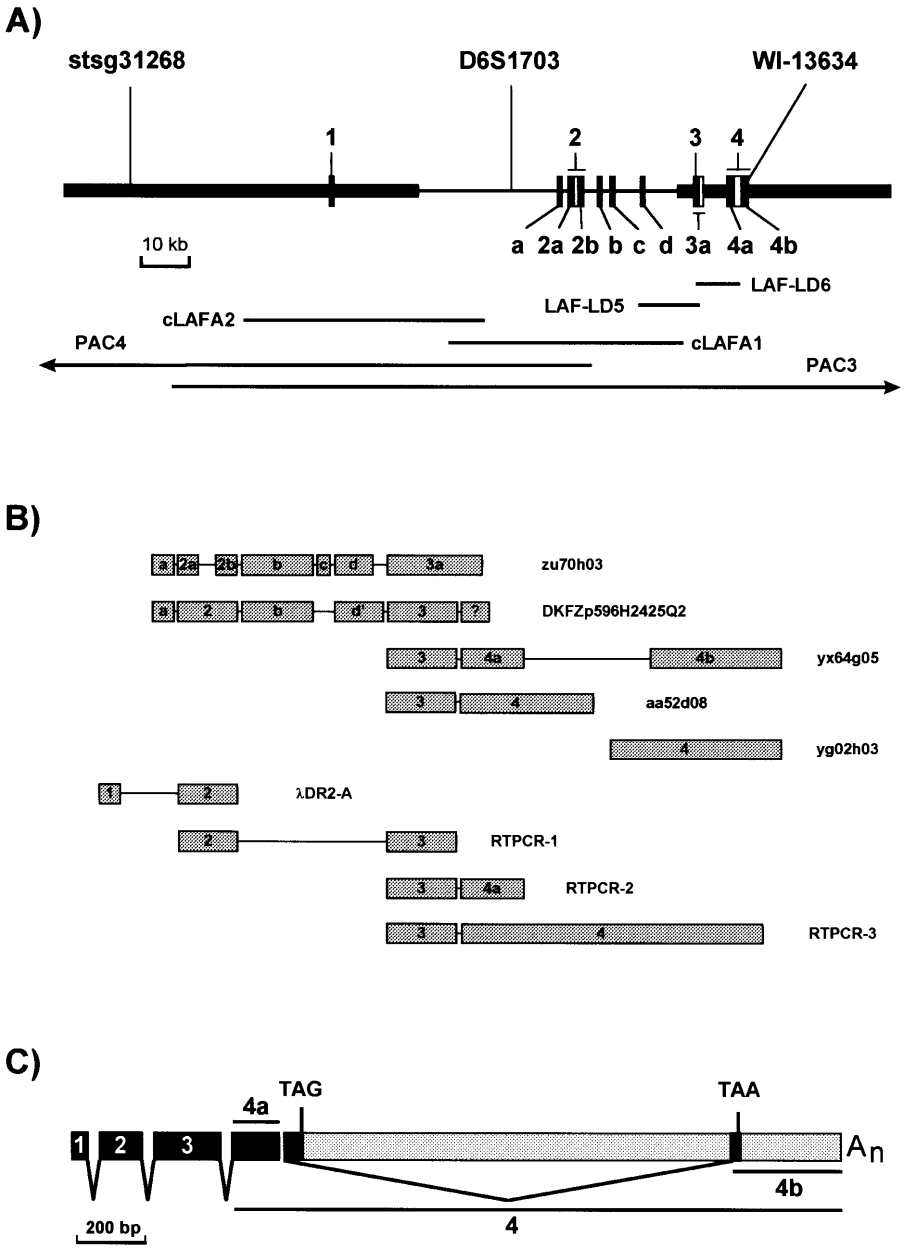

Figure 2. Genomic organization and mRNA structure of the EPM2 positional candidate gene. (**A**) Diagram of the genomic structure of the *EPM2* gene. The thick line represents the genomic DNA, in which the position of the deletion characterized in family FD is illustrated with a thin line. The exons of the EPM2 positional candidate gene are indicated with vertical bars. Exons detected in RT–PCR experiments (B) are labeled 1, 2, 3 and 4. Exons a, 2a, 2b, b, c, d, 3a, 4a and 4b were characterized in cDNA clones. The position of the human PAC and cosmid genomic clones generated in the cloning of the DNA encompassing the deletion are indicated below the map. LAF-LD5 and LAF-LD6 are PCR fragments generated by LD-PCR. (**B**) Schematic representation of the exon organization of five overlapping EST clones and four RT–PCR fragments. λDR2-A is a PCR fragment that corresponds to the 5′ end of a cDNA clone in a human fetal liver cDNA library (HL5003A; Clontech, Palo Alto, CA). For each of the clones, the exons are indicated with boxes numbered with the same code as in the genetic map. (**C**) Composite cDNA of the EPM2 positional candidate gene based on RT–PCR analysis of skeletal muscle and liver mRNA. This composite sequence is probably incomplete at its 5′ end and, thus, the translation start ATG codon has not been determined yet. This composite sequence and the deduced amino acid sequences were deposited in GenBank under accession nos AJ130763 and AJ130764.

F102) with band-shifts in exon 4 were identified. None of these band-shifts in *EPM2* exons 2, 3 and 4 were detected by SSCP in 60 healthy controls. Mendelian inheritance of the mutations was confirmed in all the EPM2 families.

Sequence analysis of the fragments presenting band-shifts revealed that in family S114, both parents were heterozygous at the *EPM2* exon 2 (Fig. 5). They did both present a normal allele, with a sequence identical to the sequence of the *EPM2* cDNA clones, and a second allele that we denoted $EPM2^{Y31fs}$. This mutated allele is characterized by an insertion of an A at nucleotide position 95, changing a tyrosine residue at position 31 (TAC) to a stop codon (TAA). The Y31fs mutation truncates LAFPTPase at the N-terminal region of the amino acid sequence and, therefore, it is considered a loss-of-function mutation. The

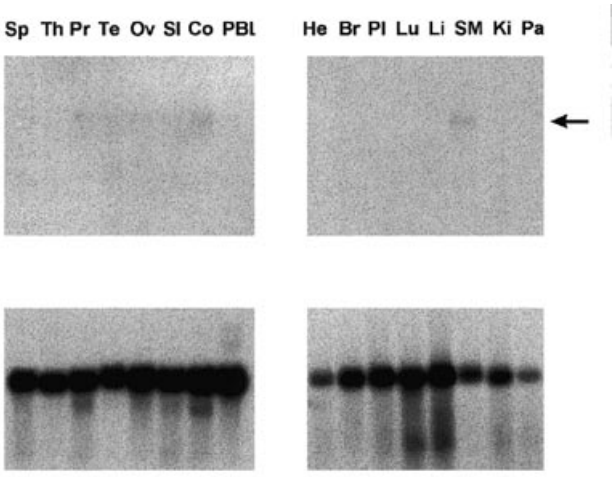

Figure 3. Expression of the *EPM2* gene. A northern blot containing poly(A)$^+$ mRNA from various adult human tissues was hybridized with probe yx64g05 (top) and GAPDH (bottom). An mRNA band of ~3 kb was detected in most of the tissues. Sp, spleen; Th, thymus; Pr, prostate; Te, testis; Ov, ovary; SI, small intestine; Co, colon; PBL, peripheral blood lymphocytes; He, heart; Br, brain; Pl, placenta; Lu, lung; Li, liver; SM, skeletal muscle; Ki, kidney; Pa, pancreas.

affected individual in family S114 is homozygous for the *EPM2*^{Y31fs} allele (Fig. 5). This segregation pattern is in full agreement with the autosomal recessive mode of transmission of EPM2, strongly suggesting that Y31fs is the causative mutation.

Another frameshift mutation (H172fs) was also found in heterozygosis in the affected individuals of a second EPM2 pedigree (F119). In addition, we found one nonsense (R160stop) and four missense (R90H, T113I, G198S and Y213N) mutations in several other EPM2 patients (Table 1).

Our *EPM2* mutational analysis is not complete, as it has been focused only on *EPM2* exons 2, 3 and 4a. Notably, we have identified 13 EPM2 chromosomes carrying a total of eight different *EPM2* mutations in 20 EPM2 pedigrees, whereas we found none in a scan of 120 normal chromosomes. We, therefore, conclude that the gene described here is the gene responsible for EPM2 and postulate that the four missense mutations that we have described here are non-functional alleles, either because they are not properly expressed or because the encoded polypeptide lacks enzymatic activity.

Autosomal recessive diseases commonly are caused by enzymatic defects which may result in the accumulation of storage material within the cells. In EPM2, an abnormal glucose polymer accumulates in diverse body tissues including the central and peripheral nervous system. Biochemical studies of isolated Lafora bodies showed that they are composed of 6% protein and 80–93% glucose. The fact that Lafora bodies can be hydrolyzed enzymatically by α-amylase indicated that they are glucose polymers (14,15). The effects of digestions with α-amylase, β-amylase and phosphorylase suggested that Lafora bodies contain glucose polymers linked with α(1→4) and α(1→6) bonds. Infrared spectroscopy studies have revealed that the deposits are not mucopolysaccharides, glycoproteins or gangliosides (14,15). Interestingly, the storage material in EPM2 is histochemically, ultrastructurally and biochemically similar to the polysaccharide that accumulates in branching enzyme deficiency (type IV glycogenosis) (16). However, branching enzyme activity was normal in brain and muscle from one patient (17). In type IV glycogenosis, an abnormal glycogen is produced as a consequence of branching enzyme deficiency. Abnormal and normal glycogen co-exist in diverse tissues including nervous tissue. As in EPM2, type IV glycogenosis patients are normal at birth. However, in type IV glycogenosis, the onset is much earlier than in EPM2. Gastrointestinal and neuromuscular symptoms predominate, with liver cirrhosis and muscular atrophy. Death usually occurs before the third year of life. The poor solubility of the abnormal glycogen appears to be the origin of the cellular injury. Similarities among the deposits of type IV glycogenosis and Lafora bodies suggest a common structure and, possibly, common etiological factors (16).

We identify here a novel gene encoding a putative PTPase, denoted LAFPTPase, that is mutated in patients with EPM2. PTPases are a heterogeneous group of enzymes involved in the regulation of diverse metabolic and development pathways. Although the mechanisms involved in the production of the Lafora bodies appear intriguing at this point, it is tempting to speculate that the putative metabolic pathway altered in EPM2 is regulated by LAFPTPase. One way by which loss of LAFPTPase function may result in the production of Lafora bodies is by inducing an imbalance between glycogen synthase and branching enzyme activities. This imbalance could result in the production of an abnormal glycogen.

Table 1. Summary of *EPM2* mutations in EPM2 patients

Family	Exon	Name[a]	Mutation	Nucleotide change[b]	Amino acid change predicted consequence
FD	2	EPM2-60kbdel	Deletion	Deletion exon 2	Truncation at exon 3
S114	2	Y31fs	Frameshift	c94insA	Truncation after Tyr31
S2	3	R90H	Missense	c271G→A	Arg90His
S12	3	T113I	Missense	c340C→T	Thr113Ile
F38/S109	4a	R160stop	Nonsense	c480C→T	Arg160stop
F119	4a	H172fs	Frameshift	c518T→CATGCA	Truncation after H172
F38/S109/F95	4a	G198S	Missense	c594G→A	Gly198Ser
F102	4a	Y213N	Missense	c639T→A	Tyr213Asn

[a]Nucleotide and amino acid positions were assigned based on the sequences depicted in Figure 4.

A)

```
(exons 1, 2, 3 and 4a)

TGGACACGTTCTGGTACAAGTTCCTGAAGCGGGAGCCGGGAGGAGAGCTCTCCTGGGAAGGCAATGGACC    70
   D  T  F  W  Y  K  F  L  K  R  E  P  G  G  E  L  S  W  E  G  N  G  P    23

TCATCATGACCGTTGCTGTACTTACAATGAAAACAACTTGGTGGATGGTGTGTATTGTCTCCCAATAGGA   140
  H  H  D  R  C  C  T  Y  N  E  N  N  L  V  D  G  V  Y  C  L  P  I  G     46

CACTGGATTGAGGCCACTGGACACACCAATGAAATGAAGCACACAACAGACTTCTATTTTAATATTGCAG   210
 H  W  I  E  A  T  G  H  T  N  E  M  K  H  T  T  D  F  Y  F  N  I  A      69

GCCACCAAGCCATGCATTATTCAAGAATTCTACCAAATATCTGGCTGGGTAGCTGCCCTCGTCAGGTGGA   280
G  H  Q  A  M  H  Y  S  R  I  L  P  N  I  W  L  G  S  C  P  R  Q  V  E    93

ACATGTAACCATCAAACTGAAGCATGAATTGGGGATTACAGCTGTAATGAATTTCCAGACTGAATGGGAT   350
  H  V  T  I  K  L  K  H  E  L  G  I  T  A  V  M  N  F  Q  T  E  W  D    116

ATTGTACAGAATTCCTCAGGCTGTAACCGCTACCCAGAGCCCATGACTCCAGACACTATGATTAAACTAT   420
 I  V  Q  N  S  S  G  C  N  R  Y  P  E  P  M  T  P  D  T  M  I  K  L     139

ATAGGGAAGAAGGCTTGGCCTACATCTGGATGCCAACACCAGATATGAGCACCGAAGGCCGAGTACAGAT   490
Y  R  E  E  G  L  A  Y  I  W  M  P  T  P  D  M  S  T  E  G  R  V  Q  M    163

GCTGCCCCAGGCGGTGTGCCTGCTGCATGCGCTGCTGGAGAAGGGACACATCGTGTACGTGCACTGCAAC   560
  L  P  Q  A  V  C  L  L  H  A  L  L  E  K  G  H  I  V  Y  V  H  C  N     186

GCTGGGGTGGGCCGCTCCACCGCGGCTGTCTGCGGCTGGCTCCAGTATGTGATGGGCTGGAATCTGAGGA   630
 A  G  V  G  R  S  T  A  A  V  C  G  W  L  Q  Y  V  M  G  W  N  L  R      209

AGGTGCAGTATTTCCTCATGGCCAAGAGGCCGGCTGTCTACATTGACGAAG                       681
K  V  Q  Y  F  L  M  A  K  R  P  A  V  Y  I  D  E                        226


(exon 4)

AGGCCTTGGCCCGGGCACAAGAAGATTTTTTCCAGAAATTTGGGAAGGTTCGTTCTTCTGTGTGTAGCCT   751
E  A  L  A  R  A  Q  E  D  F  F  Q  K  F  G  K  V  R  S  S  V  C  S  L    250

GTAG                                                                      755
  *                                                                       250

(exon 4b)

AGGCAGCTAGCCAGGACACATTTCCACTATAA                                          713
E  A  A  S  Q  D  T  F  P  L  *                                           236
```

B)

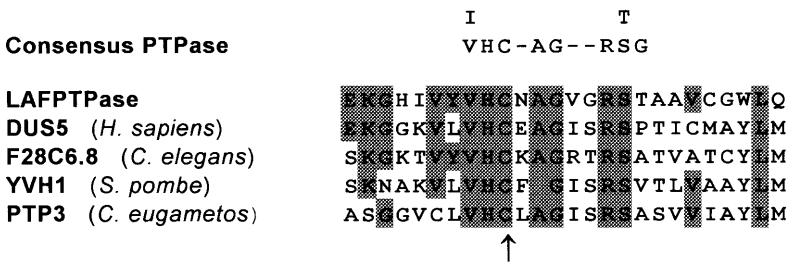

Figure 4. cDNA sequence and derived animo acid sequence of *EPM2*. (**A**) Nucleotide sequence of the cDNA corresponding to *EPM2* exons 1, 2, 3 and 4. Exon junctions are indicated with small vertical arrows. The conceptual translation of the *EPM2* ORF is shown below the cDNA sequence in one-letter code. The sequences containing the translation start ATG codon have not been found yet. (**B**) Alignment of the deduced amino acid sequence of the putative catalytic site of LAFPTPase and the catalytic site of other PTPases. Identities are shadowed. The consensus motif shared by all PTPases is shown. The critical cysteine residue is indicated with an arrow below the alignment.

In spite of the homogeneity of the EPM2 phenotype, with the presence of Lafora bodies in all affected individuals, there are ~20% of the EPM2 families in which the phenotype does not segregate with the 6q23–q25 critical region (10). The simplest explanation for this genetic heterogeneity is that other gene(s) in the same metabolic pathway is(are) altered in the EPM2 families not linked to 6q23–q25. Confirmation that the *EPM2* gene in 6q23–q25 encodes a protein with PTPase activity and the

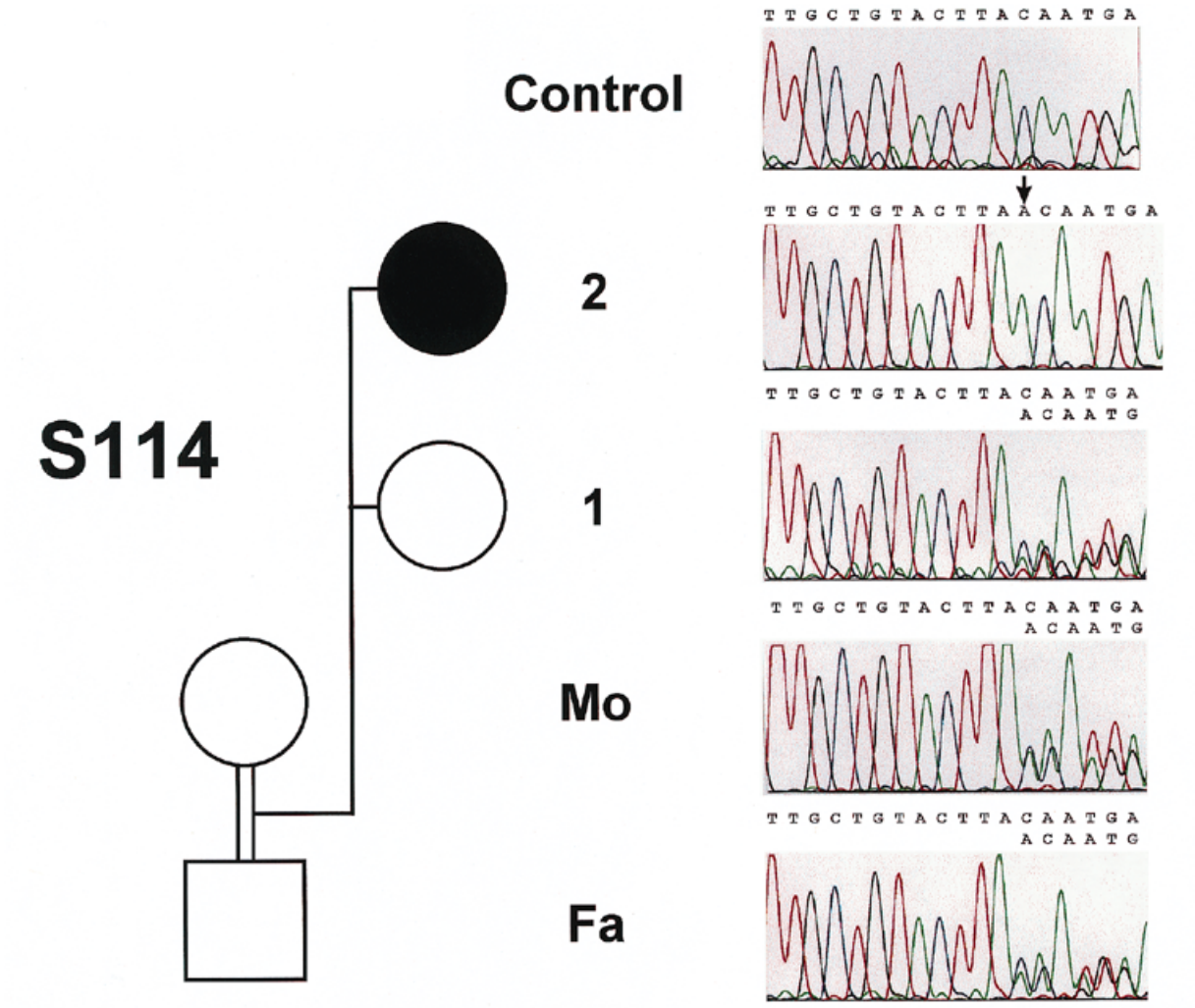

Figure 5. Segregation of the *EPM2*^{Y31fs} loss-of-function mutation in family S114. The affected individual is identified in the pedigree by a solid symbol. Relevant portions of a sequencing chromatogram are shown to illustrate the segregation of the *EPM2*^{Y31fs} allele. The insertion of an A, present in homozygosis in the affected individual, is indicated with an arrow.

identification of the corresponding substrates for the LAFPTPase should provide candidate genes for EPM2 in the families not linked to 6q23–q25.

In conclusion, the identification of the *EPM2* gene and the characterization of the corresponding enzymatic defect will increase our knowledge of the metabolic pathways involved in the accumulation of Lafora bodies and the pathogenesis of Lafora disease. It should also lead to the development of novel modalities of diagnosis and therapy for this fatal form of PME.

MATERIALS AND METHODS

Patients

The clinical diagnosis of EPM2 was based on the presentation of epilepsy, myoclonus, rapidly progressive neurological deterioration and a slow background with polyspike wave complexes in the electroencephalogram (18). In addition, we required a biopsy of skin, muscle, liver or brain showing the characteristic periodic acid–Schiff-positive Lafora bodies (19). All families included in this study were genotyped with the chromosome 6q23–q25 microsatellite markers contained in the critical region, which showed segregation with the EPM2 phenotype.

Library screening and sequencing

Two human genomic libraries (RPCI1,3-5 human PAC library and human chromosome 6 specific cosmid library, both supplied by the RZPD, German Human Genome Resource Center) and human cDNA libraries (human hippocampus library 569, human adult brain library 588 and human testis library 596, supplied by the RZPD) were screened with appropriate labeled probes. Genomic and cDNA clones were isolated by standard techniques and, if needed, subcloned into pBluescript SK$^+$ (Stratagene, La Jolla, CA). Sequencing of the cloned fragments of the *EPM2* gene was performed automatically in an ABI-377 sequencer using a dye terminator cycle sequencing kit (Perkin-Elmer). Direct sequencing of PCR products was always performed after purification of the fragments using Wizard PCR Preps DNA Purification System (Promega).

Table 2. Primers for amplification, sequencing and mutation detection

Exon	Primers for SSCP	Product size (bp)	Primers for sequencing	Product size (bp)
Exon 2	F: GTATCAGCTGCTTGAGGATA	291	F: GTATCAGCTGCTTGAGGATA	291
	R: CTTGTCCTACTTCTATGCCTA		R: CTTGTCCTACTTCTATGCCTA	
Exon 3	F: ACCAAATATCTGGCTGGGTA	230	F: CTACATGTTTTATGCAGCTCC	431
	R: TGCTCATATCTGGTGTTGGC		R: ATTTATTCCATTTCTACCATTCAT	
Exon 4a	F: GCCGAGTACAGATGCTGC	202	F: GAGAGAGCCTCTGGCCTC	483
	R: TCGTCAATGTAGACAGCCG		R: CAGAAGAACGAACCTTCCCA	

F, forward; R, reverse.

RNA isolation and RT–PCR analysis

Total RNA was isolated by the guanidinium thiocyanate method (20). Poly(A)$^+$ RNA was prepared using oligo(dT)–magnetic beads as described by the manufacturer (MPG mRNA Purification kit; CPG, NJ). Reverse transcription was performed on 1 µg of total RNA prepared from appropriate tissues using oligo(dT) as a primer and MMLV reverse transcriptase (Amersham, Cleveland, OH). One-tenth of the reaction was amplified with the corresponding primer pairs. A minus-RT control for each RNA was included in all experiments. The generated fragments were electrophoresed on 1.3% agarose gels, transferred onto nylon membranes and hybridized with the appropriate probe to confirm their identity.

Mutation analysis

SSCP analysis was performed by PCR, using total genomic DNA, as described elsewhere (21). Briefly, for SSCP analysis, amplification was performed in a total volume of 10 µl containing 40 ng of genomic DNA; 12.5 pmol of each primer; 1 U of *Taq* polymerase (Perkin-Elmer Cetus); 250 µM dATP, dGTP and dTTP; 25 µM dCTP; 1 µCi of [α-^{32}P]dCTP at 300 Ci/mmol; 1.5 mM $MgCl_2$; 50 mM KCl; and 10 mM Tris–HCl (pH 8.3). PCR conditions were one cycle at 94°C for 2 min, followed by 30 cycles of 94°C for 30s, 59°C for 1 min, and 72°C for 30s, and one cycle at 72°C for 3 min. Samples were resolved on 8% and/or 10% non-denaturing polyacrylamide gels, and exposed to Kodak XAR film with intensifying screens at –70°C for 2 h. Sequencing of the PCR fragments of the *EPM2* gene was performed automatically in an ABI-377 sequencer using a dye terminator cycle sequencing kit (Perkin-Elmer). Primers used for amplification of exons 2, 3 and 4 of the *EPM2* gene for SSCP and sequence mutation analysis are shown in Table 2.

ACKNOWLEDGEMENTS

The authors wish to thank all the patients and family members who participated in this study. We also thank Drs J. Jimenez, M.A. Peñalva, A. Silva and D. Heine for encouragement and critical reading of the manuscript, and Dr M. Robledo, Dr J. Benítez, Dr A. Díaz, Ms G. Porras, Ms S. Carnejo and Mr R. Iranmanesh for their help and contribution to this work. This work was supported by the Asociación Lafora España, the Fundación Jose Antonio de Castro, the Spanish Comisión Interministerial de Ciencia y Tecnología (SAF96/0318, SAF96/0055), the Fondo de Investigaciones Sanitarias (FIS98/0687), the Junta de Comunidades de Castilla-La Mancha and the Comunidad Autónoma de Madrid (08.6/0015/1997). P.G-G was supported by a fellowship from the Association France Lafora. In addition, this study is based upon work supported by the Fundación Conchita Rabago de Jímenez Díaz under fellowships awarded to B.A. and D.B.-V.d.B.

REFERENCES

1. Hauser, W.A. and Kurland, L.T. (1975) The epidemiology of epilepsy in Rochester, Minnesota, 1935 through 1967. *Epilepsia*, **16**, 1–66.
2. Juul-Jensen, P. and Foldspang, A. (1983) Natural history of epileptic seizures. *Epilepsia*, **24**, 297–312.
3. Berkovic, S.F., Andermann, F., Carpenter, S. and Wolfe, L.S. (1986) Progressive myoclonus epilepsies: specific causes and diagnosis. *N. Engl. J. Med.*, **315**, 296–305.
4. Lafora, G.R. (1911) Über das Vorkommen amyloider Körperchen im Innern der Ganglienzellen; zugleich Ein zum Studium der amyloiden Substanz im Nervensystem. *Virchows Arch. (Pathol. Anat.)*, **205**, 295–303.
5. Lafora, G.R. and Glueck, B. (1911) Beitrag zur Histopathologie der myoklonischen Epilepsie. *Z. Gesamte Neurol. Psychiatr.*, **6**, 1–14.
6. Harriman, D.G.F. and Millar, J.H.D. (1955) Progressive familial myoclonic epilepsy in three families: its clinical features and pathological basis. *Brain*, **78**, 325–349.
7. Lafora, G.R. (1955) Myoclonus. Physiological and pathological considerations. In *Proceedings of the Second International Congress of Neuropathology. Part I*. Excerpta Medica Foundation, Amsterdam, pp. 9–21.
8. Serratosa, J.M., Delgado-Escueta, A.V., Posada, I., Shih, S., Drury, I., Berciano, J., Zabala, J.A., Antúnez, M.C. and Sparkes, R.S. (1995) The gene for progressive myoclonus epilepsy of the Lafora type maps to chromosome 6q. *Hum. Mol. Genet.*, **4**, 1657–1663.
9. Sainz, J., Minassian, B.A., Serratosa, J.M. Gee, M.N., Sakamoto, L.M., Iranmanesh, R., Bohlega, S., Baumann, R.J., Ryan, S., Sparkes, R.S. and Delgado-Escueta, A.V. (1997) Lafora progressive myoclonus epilepsy: narrowing the chromosome 6q24 locus by recombinations and homozygosities. *Am. J. Hum. Genet.*, **61**, 1205–1209.
10. Gómez-Garre, P., Anta, B., Castro-Gago, M., Lindhout, D., Tassinari C.A., Michelucci, R., Malafosse A., Topcu, M., Grid, D., Dravet, C. and Serratosa, J. (1998) Reduction of the Lafora disease candidate gene region to a 2 cM interval in chromosome 6q24 and evidence for genetic heterogeneity. *Eur. J. Hum. Genet.*, **6**, 152 (abstract).
11. Roberts, R.G., Coffey, A.J. Bobrow, M. and Bentley, D.R. (1992) Determination of the exon structure of the distal portion of the dystrophin gene by vectorette PCR. *Genomics*, **13**, 942–950.
12. Arnold, C. and Hodgson, I. (1991) A novel approach to genomic walking. *PCR Methods Appl.*, **1**, 39–42.
13. Barford, D., Flint, A.J. and Tonks, N.K. (1994) Crystal structure of human protein tyrosine phosphatase 1B. *Science*, **263**, 1397–1404.
14. Yokoi, S., Austin, J., Witmer, F. and Sakai, M. (1968) Studies in myoclonus epilepsy (Lafora body form). I. Isolation and preliminary characterization of Lafora bodies in two cases. *Arch. Neurol.*, **19**, 15–33.

15. Sakai, M., Austin, J., Witmer, F. and Trueb, L. (1970) Studies in myoclonus epilepsy (Lafora body form). II. Polyglucosans in the systemic deposits of myoclonus epilepsy and in corpora amylacea. *Neurology*, **20**, 160–176.
16. Hers, H.-G., Hoof, F.V. and de Barsy, T. (1993) Glycogen storage disease. In Scriver, C.R., Beaudet, A.L., Sly, W. and Valle D. (eds), *The Metabolic and Molecular Bases of Inherited Disease*. MacGraw-Hill, New York, pp. 425–452.
17. Gambetti, P., Di Mauro, S., Hirt, L. and Blume, R.P. (1971) Myoclonic epilepsy with Lafora bodies. *Arch. Neurol*., **25**, 483–493.
18. Tassinari, C.A., Bureau-Paillas, M., Dalla Bernardina, B., Picornell-Darder, I., Mouren, M.C., Dravet, C. and Roger, J. (1978) La maladie de Lafora. *Rev. EEG Neurophysiol*., **8**, 107–122.
19. Van Heycop Ten Ham, M.V. (1974) Lafora disease, a form of progressive myoclonus epilepsy. In Vinken, P.J. and Bruin, G.W. (eds), *Handbook of Clinical Neurology*. North Holland, Amsterdam, Vol. 15, pp. 382–422.
20. Chomczynski, P. and Sacchi, N. (1987) Single-step method of RNA isolation by acid guanidinium thiocyanate–phenol chloroform extraction. *Anal. Biochem*., **162**, 156–162.
21. Orita, M., Iwahana, H., Kanazawa, H., Hayashi, K. and Sekiya, T. (1989) Detection of polymorphisms of human DNA by gel electrophoresis as single-strand conformation polymorphism. *Proc. Natl Acad. Sci. USA*, **86**, 2766–2770.